Marine Biology (2018) 165:119
https://doi.org/10.1007/s00227-018-3375-2

ORIGINAL PAPER

Age estimation of the oyster *Ostrea puelchana* determined from the hinge internal growth pattern

M. S. Doldan[1,2,3] · M. de Rafélis[4] · M. A. Kroeck[2,3] · M. S. Pascual[2,3] · E. M. Morsan[3]

Received: 17 October 2017 / Accepted: 18 June 2018

Abstract
A multiproxy approach was used to analyse the internal growth pattern of *Ostrea puelchana* shells. Field investigations using fluorochrome stains were performed to estimate the deposition time of the lines of irregular growth. Cathodoluminescence (CL) microscopy of the hinge area and isotopic composition analyses of shells were performed. The oxygen isotopic composition of the shells showed seasonal fluctuations across the hinge. The results of CL microscopy and stable isotopes provided the first age estimations for wild specimens of *O. puelchana*. The maximal age of analysed oysters was 4.5 years. Shell deposition occurred at temperatures above 11 °C approximately, suggesting growth slowdown and/or cessation in winter. Lines of irregular growth showed no consistent temporal pattern; these growth structures cannot be used as sclerochronological proxies of growth season or shell age. *O. puelchana* is sensitive to seasonal environmental changes, which cause changes in its carbonate structure, although the pattern is not consistent, as in other species. In this study, the age of *O. puelchana* specimens from San Matías Gulf, Patagonia, Argentina, was estimated, providing a basis for future studies on this species.

Introduction

Age is an important component to consider when trying to understand the life history and population dynamics of a species (Hastie et al. 2000; Campana 2001). Determining age in bivalves is usually based on the records of environmental events represented in their hard structures (Rhoads and Lutz 1980; Richardson 2001). When shell increments can be expressed as a function of time, they can be used to estimate the age and the growth rate of individuals (Schöne 2008). If these shell increments are weakly defined or difficult to discern with classical sclerochronology, as is the case for ostreids, alternative methods can be applied (Rhoads and Lutz 1980; Lartaud et al. 2006). Chemical stains have been effective in overcoming classical sclerochronology limitations. In this staining method, shells are artificially date marked at a given point in the life of the individual, to which subsequent growth can be related (Richardson 1990). Suitable chemical stains must be non-lethal, be easy to detect in shells, not alter the viability of marked individuals, and be retained in the carbonate structure for an appropriate period of time (Riascos et al. 2007). Chemical staining has been previously used with oysters, and manganese marking experiments have been conducted with *Crassostrea gigas* (e.g. Langlet et al. 2006; Cardoso et al. 2007; Lartaud et al. 2010b; Mouchi et al. 2013) and *Ostrea edulis* (e.g. Mouchi et al. 2013). Manganese incorporated into the shells was revealed in high-luminescence microgrowth bands under cathodoluminescence (CL) microscopy (Mouchi et al. 2013). Calcein is also a useful fluorescent growth marker that has been successfully used in marine bivalves (e.g. Kaehler and McQuaid 1999; Herrmann et al. 2009). Calcein binds

Responsible Editor: A. Checa.

Reviewed by Undisclosed experts.

✉ M. S. Doldan
msdoldan@gmail.com

[1] Consejo Nacional de Investigaciones Científicas y Técnicas (CONICET), Rivadavia 1917, C1033AAJ Ciudad Autónoma de Buenos Aires, Argentina

[2] Centro de Investigación Aplicada y Transferencia Tecnológica en Recursos Marinos "Almirante Storni" (CIMAS), Universidad Nacional del Comahue, Güemes 1030, 8520 San Antonio Oeste, Provincia de Río Negro, Argentina

[3] Escuela Superior de Ciencias Marinas, Universidad Nacional del Comahue, San Martín 247, 8520 San Antonio Oeste, Río Negro, Argentina

[4] Géosciences Environnement Toulouse, Université Paul Sabatier (UT 3), 14 av. E. Belin, 31400 Toulouse, France

Published online: 28 June 2018

to calcium and is incorporated into the growing carbonate matrix (Moran 2000). The mark fluoresces lime-green when viewed under blue light (Herrmann et al. 2009). Calcein produces a clear mark, even at low concentrations and short immersion times, and the mark is long-lasting in the field (Riascos et al. 2007). Calcein has been used with *Pinctada margaritifera* (Le Moullac et al. 2016) to measure shell deposition rates.

CL examination of bivalve shells is an alternative method that reveals the position of the internal growth lines and microstructural patterns, even when they are undetectable under transmitted light (Barbin 2013). CL refers to the emission of visible light from a material as a result of excitation by an external source of energy (an electron beam). In calcite, manganese ions (Mn^{2+}) are the principal luminescence activators emitting yellow, orange to orange-red light (~ 620 nm) (Bougeois et al. 2014), and emission intensity is positively correlated with manganese concentrations (de Rafélis et al. 2000; Langlet et al. 2006). The uptake of manganese is linked with variations in the metabolic activity of the animal and physical–chemical conditions of the surrounding environment (Barbin 2013). By exposing shells to cathode rays, it is possible to record fluctuations in the luminescence of trace elements (Lartaud et al. 2006; Cardoso et al. 2007; Lartaud et al. 2010a). Reliable estimates of shell growth can be provided as long as CL banding is validated (Barbin 2013). Therefore, if banding is seasonal, age can be determined according to the number of bands of greater intensity. The method has been used in crassostreid oysters, such as *Magallana gigas* (e.g. Langlet et al. 2006; Cardoso et al. 2007; Lartaud et al. 2010a), and in fossilized shells of *Crassostrea aginensis, Ostrea bellovacina* and of *C. virginica* (e.g. Lartaud et al. 2006). The number of low- and high-intensity bands along a transect through the hinge section corresponds to the ontogenic age of the individual (Cardoso et al. 2007; Lartaud et al. 2010a).

Sclerochemical analyses of stable isotopes are a reliable method of estimating age and growth-related characteristics in bivalve shells (Durham et al. 2017). A direct relationship between the oxygen isotope composition of both the shell carbonate and the seawater can be established when shell calcium carbonate precipitation occurs in isotopic equilibrium with seawater (Epstein et al. 1953). Precipitation under isotopic equilibrium has been demonstrated for crassostreid oysters (e.g. Kirby et al. 1998; Surge et al. 2001; Ullmann et al. 2010). Geochemical signals of biogenic carbonate have been used in recent and fossilized oysters such as *M. gigas* (e.g. Fan et al. 2011; Goodwin et al. 2013; Langlet et al. 2006; Lartaud et al. 2010a), *O. edulis* (Mouchi et al. 2013), *O. edulis* var. *lamellosa* and *M. gryphoides* (e.g. Sælen et al. 2016). The oxygen isotope composition of the shell carbonate can also be used as a paleothermometer (e.g. Kirby et al. 1998). This method is based on the premise that isotopic fractionation between shell carbonate and surrounding water is a function of environmental temperature and water composition (Fan et al. 2011).

The Puelche oyster, *Ostrea puelchana*, is a shallow, subtidal marine species native to the South Atlantic coast (between 22°53′S and 42°22′S; Creed and Kinupp 2011; Doldan et al. 2014). This is a commercially valuable flat oyster that is well researched due to its importance in aquaculture at San Matías Gulf (SMG), Northern Patagonia, Argentina (Castaños et al. 2005). *O. puelchana* is a protandric alternating hermaphrodite (Morriconi and Calvo 1979). Changeover from male to female occurs several times in its life. Large oysters (≥ 55 mm) are predominantly females (Morriconi and Calvo 1979). Gametogenesis occurs from mid-spring to late summer (mid-November to mid-March) (Morriconi and Calvo op. cit.). Embryos are incubated during a short breeding period (5–6 days; Zampatti and Pascual 1989), and settlement occurs during the warm season, from December to March (Pascual and Bocca 1988). *O. puelchana* is unique among extant oysters: large oysters (≥ 55 mm) can carry dwarf epibiotic oysters attached to a flat platform on the anterior edge of the left valve (Calvo and Morriconi 1978; Pascual et al. 1989; Shilts et al. 2007). During the spawning season, these epibiotic oysters develop a male gonad (Fernández Castro and Lucas 1987). The growth rate of the dwarf oysters is severely reduced by a chemically mediated inhibitory effect of the carrier oyster (Pascual et al. 1989). This fact leads to two demographic structures: an *apparent* demographic structure, represented by subadult oysters (≤ 55 mm) and adult oysters, and a *real* demographic structure, which incorporates the small epibiotic males (Pascual et al. 2001). Puelche oysters can be observed living in solitary or gregarious conditions. Gregarious oysters form *clusters* as a result of larvae successively settling and growing on the shell of a conspecific: the founder oyster (Morriconi and Calvo 1979). *Clusters* are typically formed of two or three oysters, but can be formed by up to nine oysters. The incidence of gregariousness differs among oyster grounds in SMG (2–50%). This finding may be a result of differences in the turnover rate or of regulatory mechanisms, such as interspecific competition or predation by chitons (Pascual et al. 2001).

Age estimation has never been explored in *O. puelchana*. Unlike other bivalves, *O. puelchana* shells lack reliable external or internal morphological indicators of annual accretionary growth. Even when internal growth lines are discernible, a clear deposition pattern has not been demonstrated. Previous studies based on farmed oysters described seasonal variations in the growth rate of *O. puelchana* (Pascual et al. 2001), which were correlated with water temperature (Fernández Castro and Bodoy 1987). Growth experiments using cultured *O. puelchana* revealed growth cessation during the cold months (Pascual and Bocca 1988).

The occurrence of 4-year-old *Leiosolenus patagonica* (bivalves that bore into oyster shells) (Bagur et al. 2013) on *O. puelchana* and the growth rate of farmed *O. puelchana* suggest it is a long-lived species (Pascual et al. 2001).

The present paper reports results of ontogenic age determination for individual *O. puelchana*, which provides new quantitative insight into the population dynamics of this species. The aims of this work were (a) to validate the periodicity of lines of irregular growth in *O. puelchana* shells, (b) to investigate whether the species shows seasonal environmental changes within the shell, and (c) to date each portion of the shell to estimate the age of the specimens.

Materials and methods

The study was carried out at SMG, Northern Patagonia, Argentina (40°50′–42°15′S, 63°5′–65°10′W Fig. 1). The gulf is a semi-enclosed basin that partially communicates with the open sea through a shallow sill (60 m depth) that limits water exchange (Rivas and Beier 1990). Water circulation in the gulf is dominated by two eddies, one with a cyclonic gyre in the north and the other with an anticyclonic gyre in the south. In spring, an intense thermohaline front divides the water into two masses with different oceanographic conditions: relatively cold and less salty waters similar to open shelf waters occur south of the front, whereas warm and salty waters occur north of the front (Piola and Scasso 1988; Gagliardini and Rivas 2004) (Fig. 1). The difference in temperature between both regions reaches 3 °C in summer. Waters from the NW and NE coasts do not mix as they are separated by long sandy ridges at the mouth of San Antonio Bay (Lanfredi and Pousa 1988). Seasonal streams drain at 41.5°S. The average tidal amplitude is 7.62 m (maximum 9.2 m). Seawater temperatures range, on average, from 10 °C in winter (August) to 18.2 °C in summer (January) at a depth of 20 m. The bottom sediment is mainly sand near the coastline and is gradually mixed with shell fragments, gravel and mud (Morsan et al. 2010). Mean annual land surface precipitation is 275 ± 108 mm (1980–2000, SMN).

Environmental records were retrieved from several sources. Sea surface temperatures (SST) for the period 1985–2007 were obtained from NOAA-NASA (www.nodc.noaa.gov). Data for monthly SST were produced by averaging the temperature at a window of 3 × 3 pixels centred at the locations of El Sótano (hereafter ES) and of Puerto Lobos (hereafter PL). Average daily water temperature recorded between 2007 and 2008 (water year: 7 September through 28 August) was registered in situ at the sea bottom at ES at 2.5 km from the coast (40°57.268S, 65°6.460W) at 6 h intervals with a temperature data logger [OpticStowAway-TidbiT (°C) OnSet ± 0.20 °C] (Fig. 2a). For the rearing experiment, seawater temperature was registered in situ throughout the year (10 December 2009 through 8 December 2010) with a second temperature data logger (OpticStowAway TidbiT) fixed to a submerged lantern net (3 m below the water surface) at 6 h intervals (Fig. 2b). Salinity was measured in water samples from Las Grutas (hereafter LG) and Caleta de los Loros (hereafter CLL) and at a location inside San Antonio Bay (hereafter SAB) in the summer of 2009–2010 and fall of 2010 (Table 1). Salinity was measured weekly from water samples from ES during 2017. Salinity values for PL were extracted from previous measurements at stations close to oyster grounds (Guerrero and Svendsen 2007).

Shell description

Shells of *O. puelchana* are solid. The right shell is flat and lamellated. The left shell is larger, lamellated and convex (Castellanos 1957). The maximum size registered was 140 mm (measured from the umbo to the opposite margin) (Pascual et al. 2001). Oyster shells are fully formed

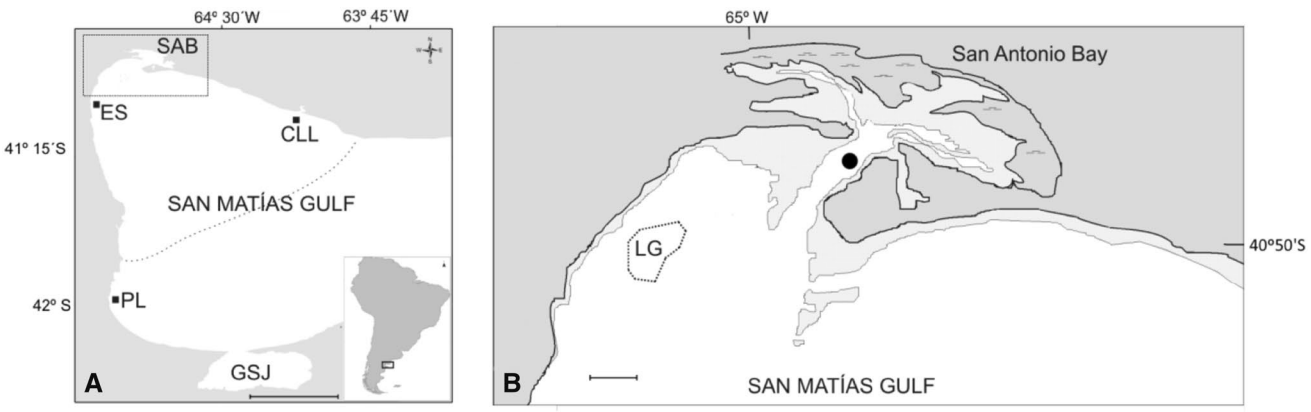

Fig. 1 **a** *Ostrea puechana* populations at San Matías Gulf, Argentina: El Sótano (ES), Caleta de Los Loros (CLL) and Puerto Lobos (PL) (Scale bar: 50 km). **b** San Antonio Bay (SAB) with location of the rack (black dot) and Las Grutas (LG) oyster population. (scale bar: 5 km)

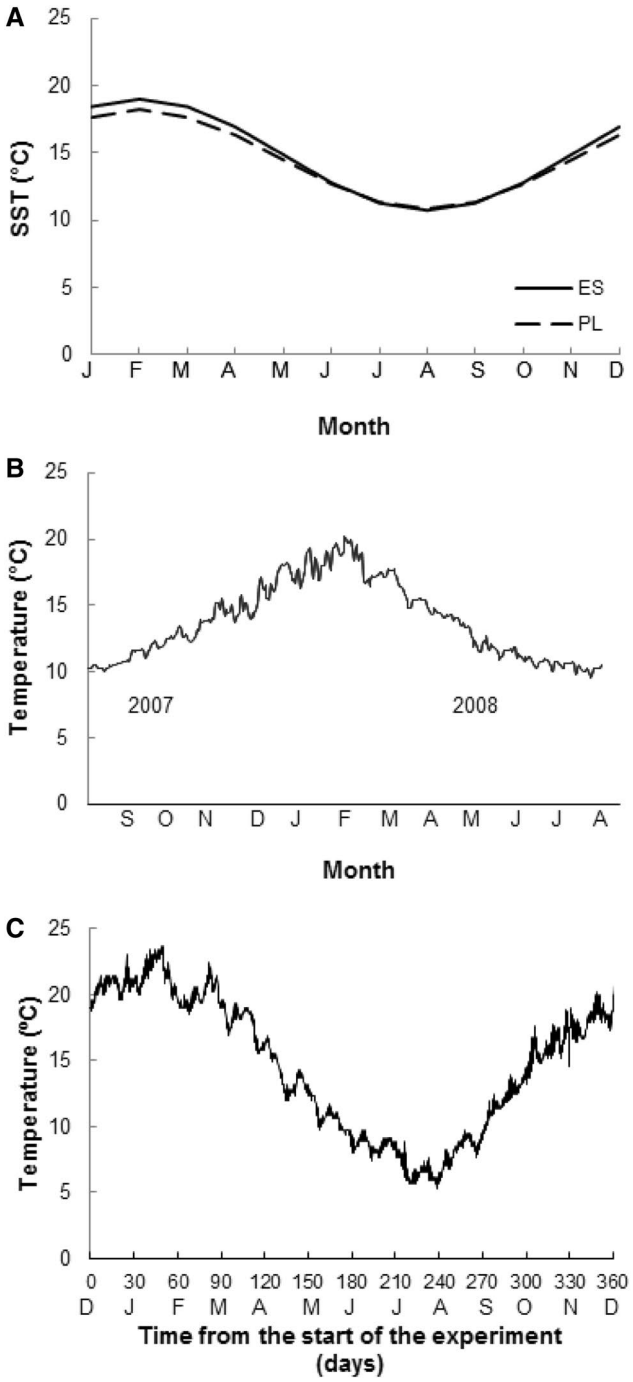

Fig. 2 **a** Annual surface sea temperature (SST) for the period 1985–2007 for El Sótano (ES) and Puerto Lobos (PL). **b** In situ bottom seawater temperature from El Sótano, from September 2007 to September 2008. **c** Seawater temperature measured by a thermobottom attached to a submerged floating rack at San Antonio Bay, Patagonia Argentina, for the period December 2009–December 2010

by calcite (Bagur et al. 2013), and two microstructures are present: foliated calcite layers and, discontinuously, chalky calcite layers (Esteban-Delgado et al. 2008). Internal growth lines are discernible in cross sections of the shell (Fig. 3). These lines were defined as lines of irregular growth (hereafter *lig*), adapting the definition of Richardson (2001) for irregular growth breaks. The author defined irregular growth breaks as interruptions in the shell deposition for a period of time as a result of environmental and/or physiological stress.

Calcein staining experiment

Oysters were collected by SCUBA divers at the LG oyster ground, SMG, Argentina (Fig. 1), in November 2009. A total of 210 oysters were selected, covering the range of shell lengths (20–120 mm). Oysters were conditioned in 650-l aquaria equipped with mesh buckets (each with 25–30 specimens). Aquaria contained filtered and aerated circulating seawater under controlled conditions (15 h light:9 h dark photoperiod, salinity 34, pH 7.2, water temperature 12–14 °C). Specimens were fed daily with a microalgae mixture (4:5:1) of *Isochrysis galbana*, *Chaetoceros gracilis* and *Tetraselmis suecica* (20 l).

A solution of 50 mg calcein (Sigma, CAS 1461-15-0) per litre was used for the staining experiment with a 6-h immersion period (following Herrmann et al. 2009). NAOH was added to return the pH of the solution to the original value. A total of 210 oysters were placed in three 100-l aquaria, and the calcein solution was slowly added. Each aquarium was placed in the dark during the staining phase to prevent light-induced degradation of the fluorochrome. After immersion in the staining solution, oysters were returned to their stocking tanks in the hatchery for 24 h. A non-treated control group ($n = 30$) was maintained in control tanks without staining solution.

Stained and control oysters were placed in three lantern nets (each net contained 25 specimens per floor) and reared in situ on a rack inside SAB (40°46.54S, 64°53.04W, Fig. 1) from December 2009 to December 2010. Lantern nets stood 3 m below the water surface. Seawater temperature was registered at 6 h intervals during the whole year. The rack was visited every 8 weeks to remove a subsample of oysters (n_{oyster} varied between 22 and 69) from the lantern nets and transferred to the laboratory (Table 2). In each visit, oyster survival was checked and fouling organisms were removed from the lantern nets and the shells (Table 2). Dead oysters and empty shells were removed from the lantern nets. At the laboratory, all oysters were measured, weighed, and carefully opened. Shells were cleaned and dried at room temperature for 48 h. In December 2010, all remaining oysters ($n = 62$) were removed from the rack and transported to the laboratory. Shells were sectioned across the longest growth axis (Fig. 3) using a Struers low-speed diamond saw (MOD13) to obtain thin shell sections (0.5–0.8 mm) of both the right and left shells. The internal section of the valve obtained from the first cut was ground and polished on a variable-speed platform using fine-grain sandpaper (up to

Table 1 Geographic and environmental data from the growing site (Bahía de San Antonio, BSA) and from the four locations under study

Location	BSA	LG	CLL	ES	PL
Latitude	40°46.7′S	40°49.33′S	41°3.42′S	40°56′S	42°S
Longitude	64°54.4′W	65°5.3′W	64°3.39′W	65°6′W	65°1′W
Depth with low tide (m)[a]	2-4	5	10	10	15
Tidal mean amplitude (m)[b]	6.71	6.71	6.04	7.3	NA
Temperature (°C)[c]					
Annual mean	14.6° (4.9°)[g]	14.6° (3.5°)[d]	15.8° (0.9°)[e]	13.9° (2.9°)[f]	13.9° (2.6°)[d]
Maximum	23.7°	21°	NA	20.2°	18.2°
Minimum	5.4°	8°	NA	9°	10.8°
Type of substrate[h]	Sand and gravel	Coarse sand and gravel	Sand, gravel and shell fragments	Sand, gravel and shell fragments	Sand[h]
Salinity range (ppm)[i]	34–38	34–36	34–35	34–36	35

Locations: Las Grutas (LG), Caleta de Los Loros (CLL), El Sótano (ES) and Puerto Lobos (PL)

[a]Measured in situ at the sample site

[b]Naval Hydrography Service of Argentina (www.hidro.gob.ar)

[c]Mean (SD) annual seabed temperature

[d]Measured with temperature logger from June 2011 to July 2014

[e]SST from satellite image of the last 10 years (NOAA www.oceancolor.gsf.nasa.gov) (Bagur et al. 2013)

[f]Measured with temperature logger from September 2007 to August 2008

[g]Measured with a temperature logger attached at a lantern from December 2009 to December 2010

[h]PL data from Márquez and Van Der Molen (2011)

[i]Measured with refractometer; PL data from Guerrero and Svendsen (2007)

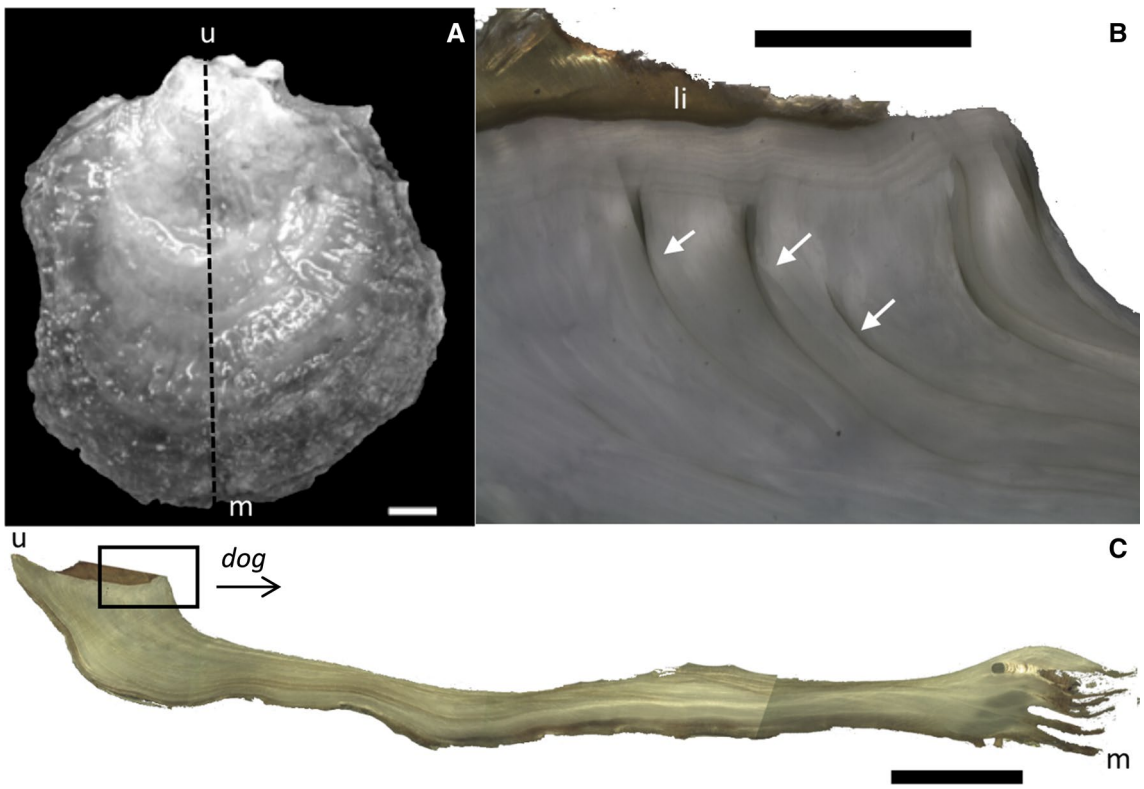

Fig. 3 *Ostrea puelchana* shell sections. **a** The right shell was cut off along the longest growth axis. Scale bar: 10.0 mm. **b** Thin shell section of the hinge exhibiting internal lines of irregular growth (*lig*, white arrows) Scale bar: 2.0 mm. **c** Polished cross section of *O. puelchana* from hinge to ventral margin of the shell. Scale bar: 10.0 mm. *dog* direction of growth; *li* ligament; *m* margin; *u* umbo

Table 2 Calcein marks at *Ostrea puelchana* hinge

Subsample ID	Date of collection of oysters	Rearing time (months)	Collected oysters (*n*)	Cumulative mortality	Oysters with calcein mark at hinge
BI	24/02/10	2.5	22	9	1
BII	28/04/10	4.5	69	22	5
BIII	23/08/10	8.5	33	29	6
BIV	05/11/10	11	13[a]	42	3[a]
BV	07/12/10	12	62	49	7

Dates of periodic sampling from the rack located at San Antonio Bay from December 2009 to December 2010

[a]Only dead oysters were removed from the lanterns in November 2010 (BIV)

P4000 grit). The polished surface was mounted on a glass slide using cyanoacrylate adhesive. Thin sections were obtained from second cuts and were ground and polished again until a uniform thickness was achieved.

Calcein marks were detected by examining each shell section under a fluorescence optical microscope (Axiolab HBO 50) under blue light (460–490 nm). If a calcein mark was observed under blue light but was not observed under red light, the thin section was photographed using digital image processing software AxioVision release 4.6.3 (2008). Growth patterns were analysed only in shells with calcein marks at the hinge region, and the number of *lig* deposited between the fluorescent band and the newer edge was counted. Periodic samplings from the lantern nets were used to estimate the deposition time of *lig*. The number of *lig* deposited during the year vs the size of the oysters was analysed with the Spearman correlation coefficient. Annual growth rates were estimated from the calcein mark to the hinge margin.

Cathodoluminescence

Four shells were selected from specimens collected live from the SMG oyster grounds in autumn 2010. The shells were named after the oyster ground they were collected from and with the specimen number: LG-70 (height = 86.95 mm); CLL-183 (height = 73.45 mm); ES-98 (height = 98.72 mm); and PL-133 (height = 89.4 mm). Shells were sectioned with a diamond saw (see methodology above) and viewed under CL (see Langlet et al. 2006; Lartaud et al. 2010a for methodologies) on a cold cathode (Cathodyne-OPEA, 15–17 kV, 250-300 µA/mm^2 under a pressure of 60 mTorr) coupled to an optical microscope and a digital camera.

Observations were made on the hinge. Microphotograph assemblages of the hinge regions following the growth axis provided a complete view of the entire hinge area of each shell. A profile of the spatial variations in luminescence (expressed in arbitrary greyscale units) along the direction of growth axis was obtained using ImageJ software (Rasband 1997–2016).

Stable isotopes

After inspection under a CL microscope, samples of carbonate for $\delta^{18}O$ analysis were drilled from three shells (CLL-183, ES-98 and PL-133). Samples were drilled at the hinge region in a transect parallel to the growth axis (Fig. 3), starting from the oldest portion of the shell. The sampling depth was 0.1 mm, and we used a 0.3-mm-diameter drill (sampling was taken at 0.08-mm intervals). The number of drilled samples varied between 22 and 32 per shell. The collected powder was acidified in 100% H_3PO_4 at 75 °C under vacuum and was analysed with a mass spectrometer for the determination of stable oxygen isotope ratios. Isotopic data are reported in conventional delta (δ) notation relative to the Vienna Pee Dee Belemnite (VPDB). The standard deviation for $\delta^{18}O$ was ± 0.10%.

All $\delta^{18}O_{shell}$ and $\delta^{13}C_{shell}$ values were plotted against the direction of growth, and the position of the *lig* was incorporated in the plot. Age was estimated based on the number of $\delta^{18}O_{shell}$ cycles. The relationship between $\delta^{18}O_{shell}$ and $\delta^{13}C_{shell}$ values was analysed.

Seawater temperature was estimated using the temperature equation from Anderson and Arthur (Lartaud et al. 2010a) for calcite where ESW (°C) = 16–4.14 $(\delta^{18}O_{shell} - \delta^{18}O_{seawater}) + 0.13\ (\delta^{18}O_{shell} - \delta^{18}O_{seawater})^2$. Since high-resolution $\delta^{18}O_{water}$ records do not exist for SMG waters, $\delta^{18}O_{seawater}$ values were obtained from the NASA Goddard Institute for Space Studies (data.giss.nasa.gov/o18data/).

Results

Calcein staining experiment

The results of the staining experiment are summarized in Table 2. A total of five subsamples were collected through the year (namely, BI, BII, BIII, BIV and BV; Table 2). Each subsample corresponded to a season: BI summer; BII autumn; BIII winter; BIV spring; BV early summer. Only dead oysters and empty shells were removed in November

2010 (BIV, Table 2). A total of 49 oysters died during the experiment (Table 2). In December 2010, all remaining oysters ($n = 62$) were removed from the rack and transported to the laboratory.

A total of approximately 150 oysters were sectioned and observed under fluorescence optical microscope. Oysters immersed in calcein solution showed visible green fluorescent thin marks. Both right and left valves showed calcein marks; however, they were not complete across the whole shell (Fig. 4). Calcein marks across the shell varied 30–60% between subsamples. Calcein staining at hinge region was even lower (5–20%). The number of *lig* secreted after the calcein mark at the hinge region varied seasonally: in the subsample of autumn (late April; rearing time: 4.5 month), most shells exhibited 2 *lig* after the calcein mark (subsample BII in Table 2; Fig. 5). The number of *lig* did not increase in the following subsamples, neither in the winter subsample (August) nor in the spring subsample (November) (rearing time 8.5 and 11 month, respectively) (subsamples BIII and BIV in Table 2; Fig. 5). The subsample BV was composed of the oysters that completed 1 year growing at the rack. Half of the oysters with a calcein mark at the hinge had 2 *lig* after it; the rest had four *lig*. According to the periodic sampling, *lig* were deposited during the warm season, from December to April. No relationship was found between the number of *lig* deposited after the 1-year experience and the oyster size (Spearman Index = 0.09; $n = 7$; $p = 0.748$). The estimated hinge growth rate of oysters larger than 50 mm was 2.78 mm/year (SD 0.61 mm).

Some oysters had dwarf males attached to the platform of the left valve. Calcein marks were recorded along the shells of the dwarf oysters (Fig. 4). The interpretation of the results was limited to the adult oysters.

Seawater temperature varied almost sinusoidally between winter and summer months, ranging from 5.4 to 23.7 °C, respectively (Fig. 2c). Seawater temperature was above 15 °C during spring and summer, while in June and July 2010 it was below 10 °C. The daily temperature cycle showed sinusoidal variations as a result of the daily tidal currents filling SAB.

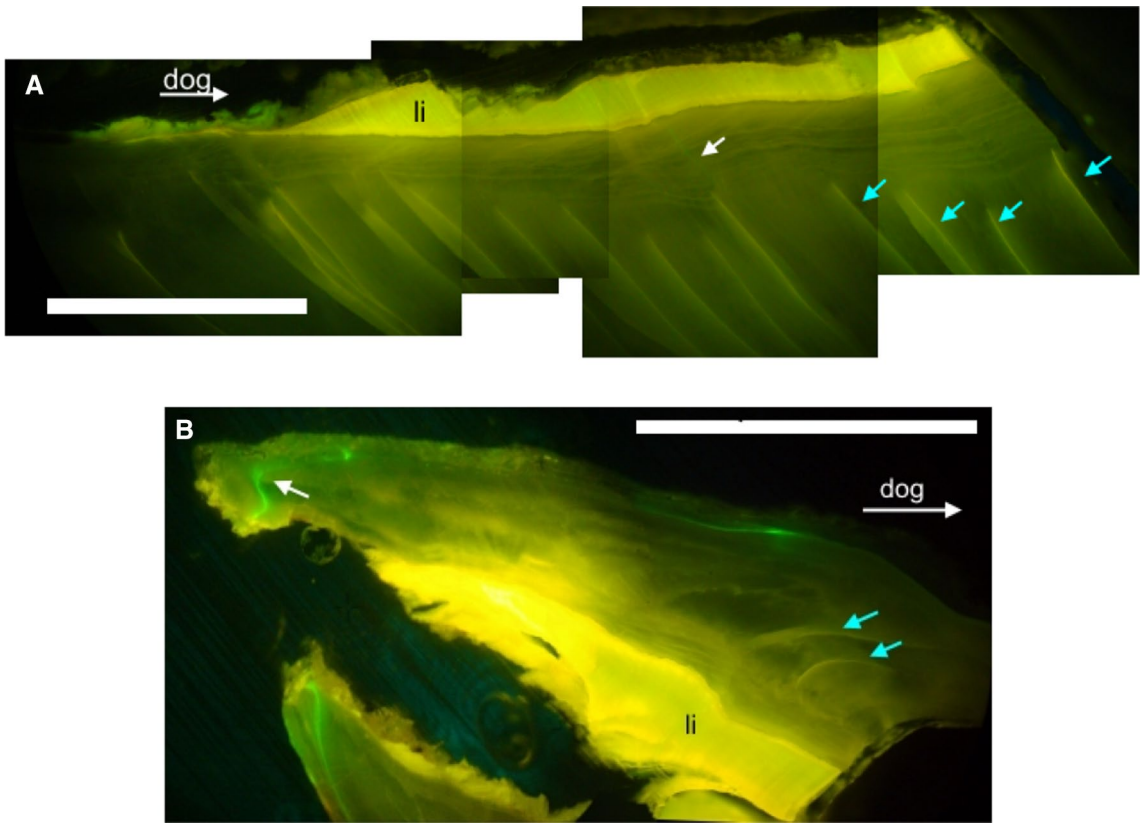

Fig. 4 Microphotograph assemblage (under blue light) of shells of *Ostrea puelchana* stained with calcein on 5 December 2009. The oysters grew during 1 year at a growing site located at San Antonio Bay. They were live collected on 10 December 2010. The incorporation of calcein was not continuous all along the shell. The white arrows indicate the calcein mark. **a** Four internal lines of irregular growth (*lig*, skyblue arrows) were deposited after the calcein mark (white arrow) in an adult oyster. Scale bar: 2 mm. **b** Lines of irregular growth (*lig*, skyblue arrows) deposited after the calcein mark in a young oyster. Scale bar: 3 mm. *dog* direction of growth; *li* ligamental area

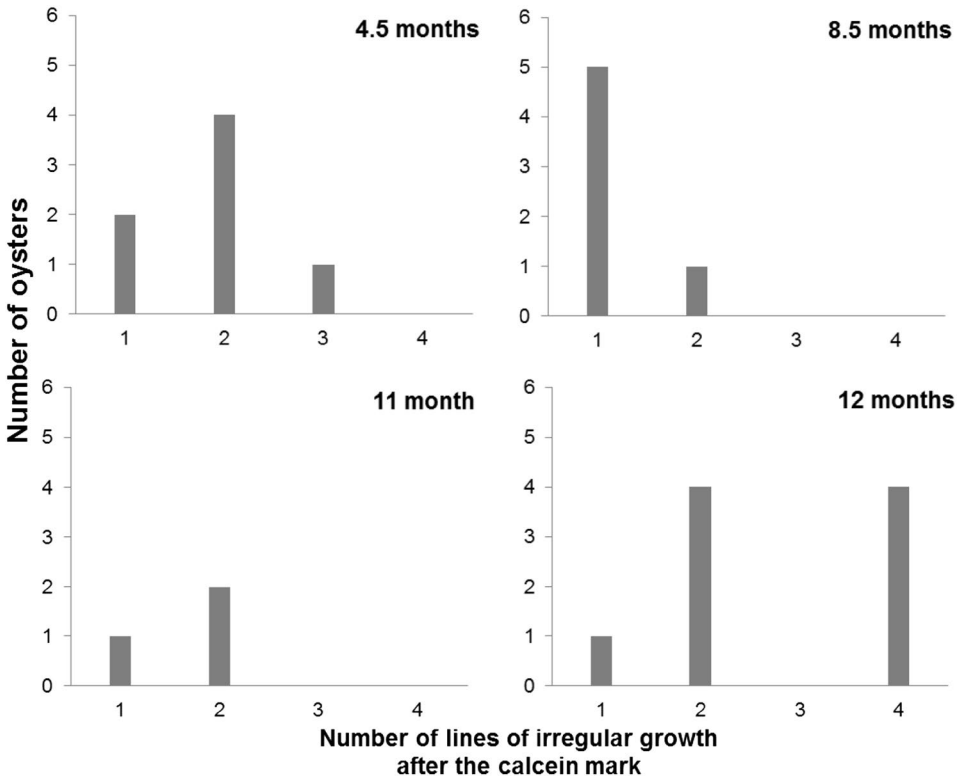

Fig. 5 Calcein staining experience. Oysters were stained and reared in lantern nets at San Antonio Bay, from December 2009 to December 2010. Number of lines of irregular growth deposited at hinge after the calcein mark for each subsample. Rearing time for each sample is at the right of each histogram

Cathodoluminescence

All four shells exhibited natural background luminescence. CL at hinge sections revealed cycling bands of alternating bright orange and dull red-violet bands (Fig. 6). In the profile of luminescence intensity, the bright orange bands corresponded to areas of high luminescence, and the dull violet bands corresponded to low-intensity luminescence. Low-luminescence dull violet areas were up to three times wider bands than high-luminescence bright orange areas (Fig. 6). The CL pattern was clearly visible in PL-133, in which a succession of four complete cycles was observed. Also a bright orange high-luminescence band of a new cycle was observed (Fig. 6). In the other shells, the pattern was not clearly observed.

In the four shells, the *lig* were recognized under CL as bright orange luminescent lines (Fig. 6). In the case of PL-133, these *lig* appeared at the beginning of each bright orange high-luminescence band. Most individuals showed weak or no luminescence in the oldest region of their hinge.

As revealed by the CL photo-assemblages, the intensity of each dull violet band was not homogeneous: some thin orange growth lines were found in this region (Fig. 6). Also, the bright orange bands showed some thin violet growth lines (Fig. 6, boxed sections). These types of periodicities have been previously identified in sclerochronological studies of mollusc bivalve shells and were related to tidal cycles (Lartaud et al. 2010a; Mouchi et al. 2013).

Stable isotope results

Oxygen isotope ratios displayed annual variations. Figure 7 shows the $\delta^{18}O$ values for each oyster plotted against the sample spot number, which represents the distance from the oldest part of the shell. Shell CLL-183 had $\delta^{18}O$ values between −0.43 and 1.21‰, shell ES-98 had a slightly broader value range (between −0.94 and 0.96‰) and shell PL-133 had lower values, between −1.89 and 0.82‰. There were gaps in the oxygen isotope composition data due to instrument malfunction.

Sinusoidal seasonal cycles were recognized in the $\delta^{18}O$ profiles of all shells, reflecting annual cycles. Salinity values were assumed to stay constant during the year at each oyster ground. Cold periods were identified as peaks in the $\delta^{18}O$ profiles followed by periods of low values (summers, Fig. 6). Given the known collection date of the oysters, it was possible to provide a sclerochronological profile for hinge growth. Specimens CLL-183 and ES-98 presented two cycles and the beginning of a new one (Fig. 7). Based on the number of $\delta^{18}O$ cycles, the ontogenic age of oysters CLL-183 and ES-98 was 2.5 years. Specimen PL-133 presented four cycles and the beginning of a new one (Fig. 7). It was estimated to be 4.5 years old (Fig. 6). Accordingly, PL-133 recruited in summer 2006, while ES-98 and CLL-183 oyster recruited in late spring 2007.

Conversion of the $\delta^{18}O_{shell}$ values into estimated seawater temperature using the Anderson and Arthur equation

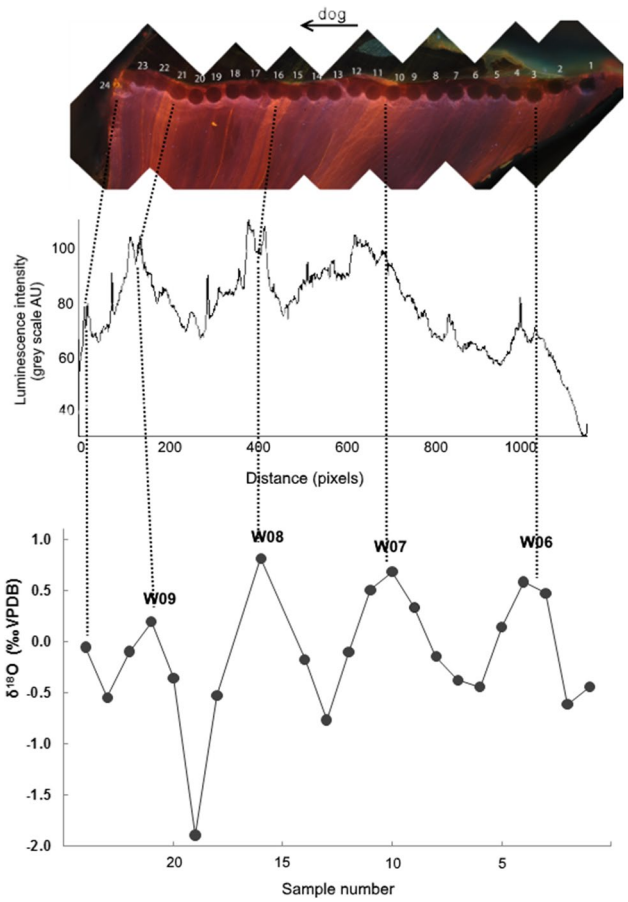

Fig. 6 Cathodoluminescence microphotograph assemblage (upper panel) of the longitudinal section of the hinge region of shell PL-133 *Ostrea puelchana* from Puerto Lobos. It showed successive areas with contrasting natural luminescence (boxed sections = micro cyclicities). Profile of luminescence intensity (middle panel), measured on the microphotograph assemblage. Profile of $\delta^{18}O_{shell}$ (lower panel). Four complete cycles are shown each corresponding to a summer (S) and winter (W) periods. dog: direction of growth

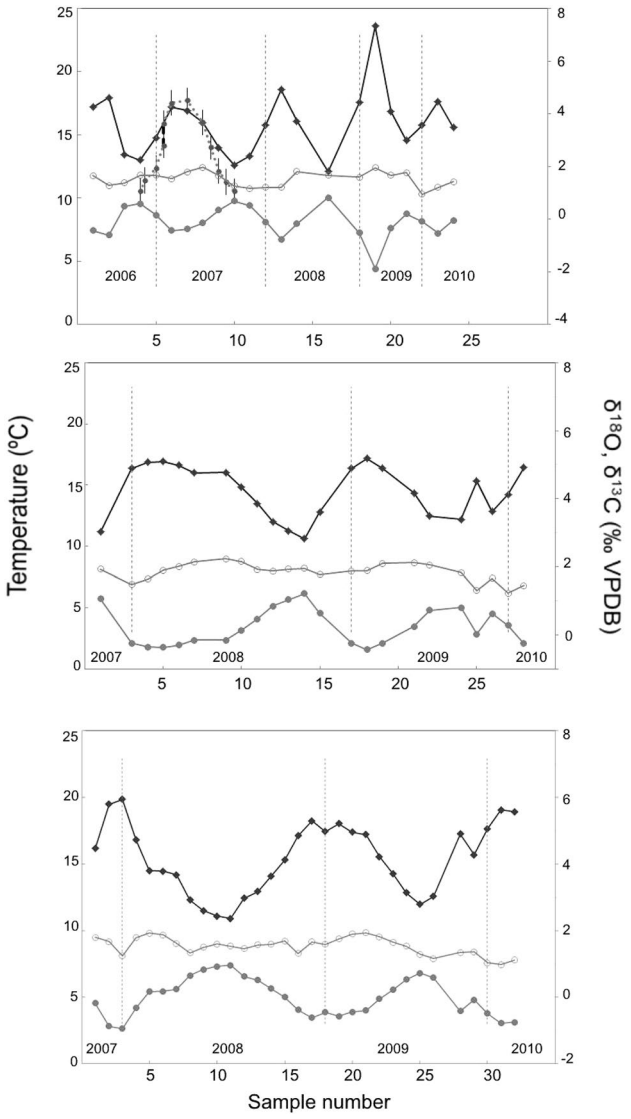

Fig. 7 Estimated seawater temperatures and $\delta^{18}O$ and $\delta^{13}C$ profiles from shell samples. Temperature was estimated from Anderson and Arthur equation (Lartaud et al. 2010a) for calcite (black line). $\delta^{18}O$ profile (grey line with grey dots) and $\delta^{13}C$ profile (grey line with white dots). Upper panel: PL-133 shell from Puerto Lobos (PL). Middle panel: CLL-183 shell from Caleta de Los Loros (CLL); ES-98 shell from El Sótano (ES; lower panel). In upper and lower panel: dotted line represents monthly mean in situ seawater temperature measured at seabed at Punta Pozos (41.6°S 64.9°W) between September 2007 and August 2008. Growth direction is towards the right, with spot #1 representing the oldest part of the shell

(Lartaud et al. 2010a) generated a range of maximum and minimum seawater temperatures. According to estimated values, the temperature amplitude varied among sites. The temperature amplitude at PL was the highest ($\delta T = 11.5$ °C; $T_{min} = 12.1$ °C; $T_{max} = 23.6$ °C), while the lowest amplitude was found at CLL ($\delta T = 6.6$ °C; $T_{min} = 10.6$ °C; $T_{max} = 17.2$ °C) (Fig. 7). These results revealed that minimum temperature for calcite deposition was 10.6 or 12 °C (Fig. 7). A comparison between estimated temperatures and in situ bottom water temperature records was possible for the ES and the PL oyster for the period 2007–2008 (Fig. 7).

The shell $\delta^{13}C$ values did not show clear seasonal variations. The values varied between 0.94 and 2.23‰ (Fig. 7). No correspondence was found between the $\delta^{18}O$ and $\delta^{13}C$ profiles.

Discussion

The puelche oyster, *O. puelchana*, is the unique native oyster of commercial importance in Argentina. During the last decades, oyster grounds of SMG have shown fluctuations: some grounds consolidated and expanded, while other grounds showed severe contraction with reduction of the abundance (Doldan et al. 2014). The estimation of the age composition

of each ground will help to understand the population dynamics of this species and to evaluate its conservation status at SMG, and the possibilities for supporting fishing pressure or aquaculture attempts. In this work, the age of wild *O. puelchana* specimens from SMG grounds, Patagonia, Argentina, was estimated for the first time.

The shells of *O. puelchana* preserve seasonal environmental records as variations in Mn^{2+} and in $\delta^{18}O_{shell}$. The microstructural pattern of Mn^{2+} content revealed by CL at the hinge consisted of a consecutive banding of a high-luminescence area followed by a low-luminescence area. The $\delta^{18}O_{shell}$ isotope profiles showed regular cycles, which were consistent with the annual seawater temperature cycle for SMG. A high-intensity peak in the CL pattern corresponded with a regional maximum of the $\delta^{18}O_{shell}$ profile, while low-intensity peaks corresponded with low $\delta^{18}O_{shell}$ values. As CL banding resulted in an annual pattern, the ontogenic age was determined according to the number of high- and low- intensity bands of each shell. CL analyses revealed intrinsic luminescence in *O. puelchana* shells. The luminescence pattern consisted of consecutive banding at the hinge region of a high-luminescence area—represented by orange narrow bands—followed by a low-luminescence area—represented by thick dull areas—. This seasonal fluctuation might be as a consequence of seasonal variations on the availability of the ion in the seawater. The manganese biochemical cycle in the Patagonian Sea shows maximum values in winter (August) and minimum values in summer (December) (Gil et al. 1989). An important result of this study is the fact that the high-luminescence areas, which are related to a high concentration of manganese in the seawaters (Langlet et al. 2006), corresponded to cold periods. In contrast, in bivalve species in the Northern Hemisphere, bright orange bands were associated with warm periods (Langlet et al. 2006). Further biogeochemical studies are needed to explore these patterns. The high-luminescence bands, secreted during the cold months, were thinner than the low-luminescence bands. The estimated temperatures from $\delta^{18}O_{shell}$ values revealed that shell deposition occurred almost all the year, except when seawater temperatures were below 11 °C approximately (10.6 °C at CL and 12 °C at PL; July to August, winter in the Southern Hemisphere). This pattern is consistent with the seasonal growth pattern previously described by Pascual and Bocca (1988). They described incremental growth in shells occurring during the warm months and growth slowdown and/or cessation during the cold months. This growth pattern has also been described for other ostreids. Shell deposition in *O. edulis* slows down during the winter months, and narrow growth lines are then formed in the umbo region; wider growth lines form during growth in summer months (Richardson et al. 1993). *Crassostrea virginica* shows slower calcification when the seawater temperature drops below 10 °C (Kirby et al. 1998). On the other hand, *Magallana gigas* can grow during cold months at slow rates (Mouchi et al. 2013). According to the estimated temperatures, *O. puelchana* shell deposition occurs when seawater temperatures are above 10°–12 °C; however, the estimated temperatures presented here should be considered with caution because they might have been slightly overestimated.

The seasonal pattern of CL intensity was clearly defined in the shell from the southernmost oyster ground (PL, 42°S, Fig. 1a). This region is influenced by the influx of cold waters from the South Atlantic Continental Shelf that balances the average temperature despite the annual gain in net heat (Gagliardini and Rivas 2004). Therefore, oceanographic conditions are more stable throughout the year, with a lower temperature and salinity, lack of stratification and a higher nitrate concentration. This leads to a noticeable growth pattern in hinges. In contrast, waters at the north of the thermohaline front present more variability, leading to weaker patterns of CL intensity. The understanding of this spatial variability is of critical importance due to its consequence in growth pattern differences among oyster grounds.

At a smaller observation scale, each high- and low-luminescence band was composed of a series of closely spaced fine growth bands, suggesting cyclicities within each growing season. Cycles with fortnightly and/or monthly periodicities have been described for bivalve shells. Growth patterns with a 7-day periodicity were found in the *Crassostrea* (=*Magallana* at present) genus, reflecting tidal patterns (Langlet et al. 2006). Mouchi et al. (2013) identified lunar and semi-lunar periodicities in the growth patterns in juvenile *M. gigas* and a lunar periodicity for adult *O. edulis*. In addition, SMG tidal and wind regimes can make the seawater temperature to drop in a couple of hours. In Fig. 2c, monthly temperature cycles are visible, some of them with a temperature range up to 4°. Future studies will focus on fluctuations in luminescence in *O. puelchana* at a high-resolution temporal scale to determine the periodicity of these cycles.

The maximum age for the oysters analysed in this study was estimated to be 4.5 years. Due to the environmental variability of the SMG grounds, stable isotopes resulted to be the conservative ageing tool. However, as some isotopic values were missing in the stable isotope profiles, life span could potentially be longer. Oysters are long-lived bivalves: maximum age estimates for *O. edulis* was 26–27 years (Stenzel 1971), whereas *C. virginica* can live for 10–20 years (Powell et al. 2013). CL analysis revealed that shell hinge records the whole shell history of *O. puelchana*. CL is a suitable technique to estimate the age of large subsamples of oysters from natural ground. It has previously been used to estimate the age of *M. gigas* subsample $^{>}$200 oysters (Cardoso et al. 2007). On the other hand, calcein staining resulted in an expensive and very high time-consuming experience, involving great logistic

efforts. Unfortunately, calcein experience gave rise lower-than-expected results: 5–20% oysters showed calcein marks at hinge. This could be attributed to a short immersion time in the fluorochrome solution. Nevertheless, calcein staining gave information about the deposition time of the *lig*. The results of the 1-year growing experience indicated that the number of annual *lig* varied between 2 and 4, and that they were deposited between December and April (summer and early autumn in the Southern Hemisphere). In agreement with that, some *lig* were recognized at the beginning of a high-luminescence band at the CL image, supporting the seasonal pattern. Nevertheless, the lack of a consistent pattern resulted in these lines not being useful as sclerochronological markers. Numerous environmental factors influence growth at the growing site, and lantern nets were placed in a dynamic and highly productive location such that growth may have been favoured. Further studies are likely to provide new insights into the deposition time of *lig*.

Future estimates of age for the entire *O. puelchana* population in SMG will allow a clearer interpretation of the population dynamics of this species in Patagonian gulfs. Comparison of demographic structures among oyster grounds and evaluations of the variability of various biological processes (growth rate, sexual transition, mortality, recruitment) would also be possible. This variability is of critical importance from the point of view of conservation and management of the species due to the major changes that have occurred over the last 15 years. For example, oyster grounds disappeared in the NW of SMG by the end of the 1990s, and populations have settled south of the historical range of oysters (Doldan et al. 2014).

The present paper serves as a basis for future studies on *O. puelchana* and offers novel possibilities for estimating age to help understand the population dynamics of this species. The methodologies applied in this study will allow us to estimate the age for the entire *O. puelchana* population and to describe the *real* demographic structure of *O. puelchana*. Additionally, it will be possible to investigate differences in the growth rates between isolated and clustered oysters and to describe the longevity of dwarf males and the life span of paired carrier oyster and epibiotic males and to assess the variability in biological processes between populations (e.g. growth, sexual reversal). This variability is especially important for conservation and management efforts, particularly after the fluctuations in abundance that have been observed in the oyster grounds of SMG during the last decades (Doldan et al. 2014).

Conclusions

Ostrea puelchana records environmental changes within its carbonate structure, and shell deposition occurs during the entire year when seawater temperatures are above 10°–12 °C (winter). CL analysis revealed intrinsic luminescence in *O. puelchana* shells. The $\delta^{18}O_{shell}$ isotope profiles showed regular cycles, which were consistent with the annual cycle of the seawater temperature of SMG. The combination of methods permitted estimations of the age of wild specimens of *O. puelchana* for the first time.

The internal *lig* cannot be used as sclerochronological markers because they do not show a season-specific deposition patterns.

Age is an important component to understanding the life history and population dynamics of *O. puelchana*, and the present paper represents a basis for future studies in this species.

Acknowledgements The calcein experiment was supported by projects PICT 2007-1338 and PICT 2006-1674 from Agencia Nacional de Promoción Científica y Técnica, Argentina, and by projects M019 and M025 from Universidad Nacional del Comahue. We are grateful to CULMAR S.A. for allowing us to use the rack for the growing experiment. We offer our special thanks to Dr. Saba and UNPSJB-CENPAT at Puerto Madryn for the fluorescence microscope and also our special thanks to all colleagues at CRIAR (criadero) for their assistance with the lantern nets and tanks maintenance. MSD thanks M. Herrmann for staining advice and M. Brögger for calcein pictures. The present work was part of the PhD dissertation of MSD. Seawater samples for salinity measurement and in situ seawater temperature data were provided by the Programa de Monitoreo de calidad ambiental de las zonas de producción of CIMAS, Secretaría de Agricultura, Ganadería y Pesca of Provincia de Rio Negro, Argentina. CL and isotope analyses were performed at Laboratoire Biominéralisations et Environnements Sédimentaires de la Maître de Conférences Université Pierre et Marie Curie, Paris, France.

Compliance with ethical standards

Conflict of interest The authors have no conflict of interest to declare.

Research involving human participants and/or animals All applicable international, national, and/or institutional guidelines for the care and use of animals were followed.

References

Bagur M, Richardson CA, Gutiérrez JL, Arribas LP, Doldan MS, Palomo MG (2013) Age, growth and mortality in four populations of the boring bivalve *Lithophaga patagonica* from Argentina. J Sea Res 81:49–56

Barbin V (2013) Application of cathodoluminescence microscopy to recent and past biological materials: a decade of progress. Miner Petrol 107:353–362

Bougeois L, de Rafélis M, Reichart GJ, de Nooijer LJ, Nicollin F, Dupont-Nivet G (2014) A high resolution study of trace elements and stable isotopes in oyster shells to estimate Central Asian Middle Eocene seasonality. Chem Geol 363:200–212

Calvo J, Morriconi ER (1978) Epibiontie et protandrie chez *Ostrea puelchana*. Haliotis 9:85–88

Campana SE (2001) Accuracy, precision and quality control in age determination, including a review of the use and abuse of age validation methods. J Fish Biol 59:197–242

Cardoso JFMF, Langlet D, Loff JF, Martins AR, Witte JIJ, Santos PT, van der Veer HW (2007) Spatial variability in growth and reproduction of the Pacific oyster *Crassostrea gigas* (Thunberg, 1793) along the west European coast. J Sea Res 57:303–315

Castaños C, Pascual MS, Agulleiro I, Zampatti E, Elvira M (2005) Brooding pattern and larval production in wild stocks of the puelche oyster, *Ostrea puelchana* D'orbigny. J Shellfish Res 24:191–196

Castellanos Z (1957) Contribución al conocimiento de las ostras del litoral Argentino (*O.puelchana* y *O.spreta*). Min Agric Gan Nac, Argentina

Creed JC, Kinupp M (2011) Small scale change in mollusk diversity along a depth gradient in a seagrass bed off Cabo Frio (Southeast Brazil). Braz J Oceanogr 59:267–276

de Rafélis M, Renard M, Emmanuel L, Durlet C (2000) Apport de la cathodoluminiscence à la connaissance de la spéciation du manganèse dans les carbonates pélagiques. CR Acad Sci Sér 2a 330:391–398

Doldan MS, Morsan EM, Zaidman PC, Kroeck MA (2014) Analysis of large-scale spatio-temporal trends of *Ostrea puelchana* beds in Northern Patagonian gulfs, Argentina. Mar Environ Res 101:196–207

Durham SR, Gillikin DP, Goodwin DH, Dietl GP (2017) Rapid determination of oyster lifespans and growth rates using LA–ICP–MS line scans of shell Mg/Ca ratios. Palaeogeogr Palaeoclimatol Palaeoecol. https://doi.org/10.1016/j.paleo.2017.06.013

Epstein S, Buchsbaum R, Lowenstam HA, Urey HC (1953) Revised carbonate-water isotopic temperature scale. Geol Soc Am Bull 64:1315–1326

Esteban-Delgado FJ, Harper EM, Checa AC, Rodríguez-Navarro AB (2008) Origin and expansion of foliated microstructure in Pteriomorph Bivalves. Biol Bull 214:153–165

Fan C, Koeniger P, Wang H, Frechen M (2011) Ligamental increments of the mid-Holocene Pacific oyster *Crassostrea gigas* are reliable independent proxies for seasonality in the western Bohai Sea, China. Palaeogeogr Palaeoclimatol Palaeoecol 299:437–448

Fernández Castro N, Bodoy A (1987) Growth of the oyster, *Ostrea puelchana* (D'Orbigny), at two sites of potential cultivation in Argentina. Aquaculture 65:127–140

Fernández Castro N, Lucas A (1987) Variability in the frequency of male neoteny in *Ostrea puelchana* (Mollusca: Bivalvia). Mar Biol 96:359–365

Gagliardini DA, Rivas AL (2004) Environmental characteristics of San Matías Gulf obtained from LANDSAT-TM and ETM + data. Gayana (Concepción) 68:186–193

Gil MN, Sastre V, Santinelli N, Esteves JL (1989) Metal content in seston from the San José Gulf, Patagonia, Argentina. Bull Environ Contam Toxicol 43:337–341

Goodwin DH, Gillikin DP, Roopnarine PD (2013) Preliminary evaluation of potential stable isotope and trace element productivity proxies in the oyster *Crassostrea gigas*. Palaeogeogr Palaeoclimatol Palaeoecol 373:88–97

Guerrero E, Svendsen GM (2007) Resultados preliminares de dos campañas oceanográficas (Golfos NORPAT-2007 1 y 2) en los Golfos San Matías y San José. Informe Técnico Interno IBMP 9/07, 16 pp

Hastie LC, Young MR, Boon PJ (2000) Growth characteristics of freshwater pearl mussels, *Margaritifera margaritifera* (L.). Freshw Biol 43:243–256

Herrmann M, Lepore ML, Laudien J, Arntz WE, Penchaszadeh PE (2009) Growth estimations of the Argentinean wedge clam *Donax hanleyanus*: a comparison between length-frequency distribution and size-increment analysis. J Exp Mar Bio Ecol 379:8–15

Kaehler S, Mcquaid CD (1999) Use of the fluorochrome calcein as an in situ growth marker in the internal mussel *Perna perna*. Mar Biol 133:455–460

Kirby M, Soniat TM, Spero HJ (1998) Stable isotope sclerochronology of Pleistocene and recent oyster shells (*Crassostrea virginica*). Palaios 3:560–569

Lanfredi NW, Pousa JL (1988) Mediciones de corrientes, San Antonio Oeste, Provincia de Río Negro. 13 pp. Informe Inédito, Instituto de Biología Marina y Pesquera "Almirante Storni"

Langlet D, Alunno-Bruscia M, de Ráfelis M, Renard M, Roux M, Shein E, Buestel D (2006) Experimental and natural cathodoluminescence in the shell of *Crassostrea gigas* from Thau lagoon (France): ecological and environmental implications. Mar Ecol Prog Ser 317:143–156

Lartaud F, Langlet D, de Rafelis M, Emmanuel L, Renard M (2006) Mise en evidence de rythmicité saisonnière dans la coquille des huîtres fossiles *Crassostrea aginensis* Tournouer, 1914 (Aquitanien) et *Ostrea bellovacina* Lanmarck, 1806 (Thanétien). Approche par cathodoluminiscence et par sclérochronologie. Geobios 39:845–852

Lartaud F, Emmanuel L, de Ráfelis M, Ropert M, Labourdette N, Richardson CA, Renard M (2010a) A latitudinal gradient of seasonal temperature variation recorded in oyster shells from the coastal waters of France and The Netherlands. Facies 56:13–25

Lartaud F, de Rafelis M, Ropert M, Emmanuel L, Geairon P, Renard M (2010b) Mn labelling of living oysters: Artificial and natural cathodoluminescence analyses as a tool for age and growth rate determination of *C.gigas* (Thunberg, 1793) shells. Aquaculture 300(1–4):206–217

Le Moullac G, Soyez C, Vidal-Dupiol J, Belliard C, Fievet J, Sham-Koua M, Lo-Yat A, Saulnier D, Gaertner-Mazouni N, Gueguen Y (2016) Impact of pCO_2 on the energy, reproduction and growth of the shell of the pearl oyster *Pinctada margaritifera*. Estuar Coast Shelf Sci 182:274–282

Márquez F, Van Der Molen S (2011) Intraspecific shell-shape variation in the razor clam *Ensis macha* along the Patagonian coast. J Molluscan Stud 77(2):123–128. https://doi.org/10.1093/mollus/eyq044

Moran AL (2000) Calcein as a marker in experimental studies newly-hatched gastropods. Mar Biol 137:893–898

Morriconi ER, Calvo J (1979) Alternative reproductive strategies of *Ostrea puelchana*. Hydrobiologia 185:195–203

Morsan EM, Zaidman PC, Ocampo Reinaldo M, Ciocco N (2010) Population structure, distribution and harvesting of southern geoduck, *Panopea abbreviata*, in San Matías Gulf (Patagonia, Argentina). Sci Mar 74:763–772

Mouchi V, de Rafelis M, Lartaud F, Fialin M, Verrecchia EP (2013) Chemical labelling of oyster shells used for time-calibrated high-resolution Mg/Ca ratios: a tool for estimation of past seasonal temperature variations. Palaeogeogr Palaeoclimatol Palaeoecol 373:66–74

Pascual MS, Bocca AH (1988) Cultivo experimental de la ostra puelche, *Ostrea puelchana* D'Orb., en el Golfo San Matías, Argentina. In: Verreth J, Carrillo M, Zanuy S, Huisman EA (eds) Aquaculture research in Latin America. Pudoc, Wageningen, pp 329–345

Pascual MS, Iribarne OO, Zampatti E, Bocca AH (1989) Female-Male interaction in the breeding system of the puelche oyster *Ostrea puelchana* d'Orbigny. J Exp Mar Biol Ecol 132:209–219

Pascual MS, Zampatti E, Iribarne O (2001) Population structure and demography of the puelche oyster (*Ostrea puelchana*, D'Orbigny, 1841) grounds in Northern Patagonia, Argentina. J Shellfish Res 20:1003–1010

Piola AR, Scasso LM (1988) Circulación en el Golfo San Matías. Geoacta 15:33–51

Powell EN, Morson JM, Ashton-Alcox KA, Kim Y (2013) Accommodation of the sex-ratio in eastern oysters *Crassostrea virginica* to variation in growth and mortality across the estuarine salinity gradient. J Mar Biol Assoc UK 93:533–555

Rasband W (1997–2016) ImageJ, U.S. National Institutes of Health, Bethesda, Maryland, USA. https://imagej.nih.gov/ij/

Rhoads DC, Lutz RA (1980) Skeletal growth of aquatic organisms. Plenum, New York

Riascos J, Guzmán N, Laudien J, Heilmayer O, Oliva M (2007) Suitability of three stains to mark shells of *Concholepas concholepas* (Gastropoda) and *Mesodesma donacium* (Bivalvia). J Shellfish Res 26:43–49

Richardson CA (1990) Tidal rhythms in the shell secretion of living Bivalves. In: Brosche P, Sündermann J (eds) Earth's rotation from Eons to Days. Springer, Berlin, Heidelberg

Richardson CA (2001) Molluscs as archives of environmental change. Oceanogr Mar Biol 39:103–164

Richardson CA, Collis SA, Ekaratne K, Dare P, Key D (1993) The age determination and growth rate of the European flat oyster, *Ostrea edulis*, in British waters determined from acetate peels of umbo growth lines. ICES J Mar Sci 50:493–500

Rivas A, Beier E (1990) Temperature and salinity fields in the North-patagonic Gulfs. Oceanol Acta 13:15–20

Sælen G, Lunde IL, Porten KW, Braga JC, Dundas SH, Ninnemann US, Ronen Y, Talbot MR (2016) Oyster Shells as recorders of short-term oscillations of salinity and temperature during deposition of coral bioherms and reefs in the Miocene Lorca Basin, SE Spain. J Sediment Res 86:637–667

Schöne BR (2008) The curse of physiology challenges and opportunities in the interpretation of geochemical data from mollusk shells. Geo Mar Lett 28:269–285

Shilts MH, Pascual MS, Foighil DÓ (2007) Systematic, taxonomic and biogeographic relationships of Argentine flat oysters. Mol Phylogenet Evol 44:467–473

Stenzel HB (1971) Oysters. In: Moore RC (ed) Treatise on invertebrate paleontology, Part N, Bivalvia. Geological Society of America, Boulder, pp N953–N1224

Surge D, Lohmann KC, Dettman DL (2001) Controls on isotropic chemistry of the American oyster, *Crassostrea virginica*: implications for growth patterns. Palaeogeogr Palaeoclimatol Palaeoecol 172:283–296

Ullmann CV, Wiechert U, Korte C (2010) Oxygen isotope fluctuations in a modern North Sea oyster (*Crassostrea gigas*) compared with annual variations in seawater temperature: implications for palaeoclimate studies. Chem Geol 277:160–166

Zampatti E, Pascual MS (1989) Larval rearing, nursery growing and implantation at oyster parks of the Argentinian oyster, *Ostrea puelchana* D'Orb. Laboratoire de Pathologie et de Génétique des Invertébrés Marine. Technical report. IFREMER. La Tremblade. France